Lightweight design of peanut sowing machine frame based on finite element analysis

Yan Yu, Linsong Diao, Dongwei Wang, Jiasheng Wang*, Xiaomin Wang, Xiaozhi Tan, Dazhi Yi
(*College of Mechanical and Electrical Engineering, Qingdao Agricultural University, Qingdao 266109, China*)

Abstract: In order to reduce the weight and energy consumption of the whole machine against the heavy mechanical structure and excessive strength redundancy in current small-scale peanut seeders with one ridge and two rows, a finite element model of the frame was established and the static finite element analysis and modal analysis were conducted with ANSYS Workbench. Sensitivity analysis that focuses on the size of intermediate support beams and other components was performed so as to set up a multi-objective optimization model. Then a size optimization and multi-objective optimization collaborative scheme was adopted so that the target was optimized by the Seagull Optimization Algorithm (SOA) to obtain the optimal solution. Based on the results of the finite element analysis, the mechanical structure of the peanut seeder was optimized for lightweight design. Furthermore, response surface plots and static structural analysis were applied for validation. It turned out that the maximum stress of the optimized structure was less than the allowable stress; the weight of the frame reduced by 32.5% after optimization; and the first-order natural frequency did not coincide with the engine input speed or working speed, thus no resonance will occur. Field experiments showed that the qualified rate of row spacing was ≥96% when operating at different speeds of different types of seeders; The seeding depth operation performance was stable, with an average qualified rate of seeding depth of ≥92%; The performance of the seeders was also stable and reliable due to the lightweight prototype structure. The research outcomes can provide an effective technical reference and theoretical basis for the lightweight design of peanut seeders and for its continuous improvement as well in the future.

Keywords: peanut sowing machine, multi-objective optimization, lightweight design, finite element analysis, optimization
DOI: 10.25165/j.ijabe.20231603.8211

Citation: Yu Y, Diao L S, Wang D W, Wang J S, Wang X M, Tan X Z, et al. Lightweight design of peanut sowing machine frame based on finite element analysis. Int J Agric & Biol Eng, 2023; 16(3): 120–129.

1 Introduction

The overall weight of a one-ridge two-row peanut sowing machine directly affects its working efficiency and power consumption[1]. The frame of a peanut seeder machine, a key bearing component whose weight accounts for a major portion of the total machine's, plays an important role in the stability and reliability of the seeder's sowing performance[2]. Due to the influence of terrain, it is required for the peanut seeder machine to feature small size, light weight, and stable working performance. Therefore, the lightweight design of the seeder machine frame is of great significance based on the requirements for machine usage and structural stability[3-5]. For the lightweight design of mechanical products, its techniques mainly involve three aspects: structure design, new materials, and new manufacturing processes. Reasonable structural design is the most direct and reliable method for lightening mechanical products[6]. The lightweight mechanical structures provides a solution for reducing the energy consumption of agricultural production and the development of new energy agricultural machinery.

With the continuous development of technology and the upgrading of the information industry, new computer-aided design software is also entering the field of agriculture[7]. The application of assistant design software such as CAD/CAE cooperated with optimized design algorithms has become a new trend in the research and development of agricultural machinery design. Cao et al.[8] applied Solidworks software for parametric modeling and its build-in simulation calculation module to conduct a static structure analysis of the central transmission drum frame in the belt conveyor. Chen et al.[9] utilized ModalVIEW software to identify the modal parameters of each order and made modal analysis of a combined harvester cutting platform. By conducting finite element analysis on the harvester cutting platform, the modal inherent frequency was obtained, which was recognized and compared to optimize a structural design that could avoid harvester resonance and achieve weight reduction. Liao et al.[10,11] and Zhou et al.[10,11] conducted static mechanics analysis, sensitivity analysis, and modal analysis respectively on the machine frame. They established a multi-objective optimization design model and obtained the best machine frame structure design scheme. The machine frame was effectively designed and optimized, making the structure more lightweight while ensuring the stability of the frame structure. Currently, the methods used in agricultural machinery design in China are more modernized, but the design and research on peanut planting machines mainly focus on planting, fertilizing, and other

Received date: 2023-03-02 **Accepted date:** 2023-05-14
Biographies: Yan Yu, PhD, Associate Professor, research interest: intelligent agricultural equipment, Email: 83518691@qq.com; **Linsong Diao**, MS candidate, research interest: agricultural machinery design and control, Email: diaolinsong@163.com; **Dongwei Wang**, PhD, Professor, research interest: intelligent agricultural equipment, Email: w88030661@163.com; **Xiaomin Wang**, MS candidate, research interest: intelligent detection and control, Email: 2298014546@qq.com; **Xiaozhi Tan**, MS candidate, research interest: intelligent detection and control, Email: 384461662@qq.com; **Dazhi Yi**, MS candidate, research interest: agricultural machinery design and control, Email: 2406677654@qq.com
***Corresponding author: Jiasheng Wang**, PhD, Professor, research interest: agricultural machinery and equipment. College of Electrical and Mechanical Engineering, Qingdao Agricultural University, Qingdao 266109, China. Tel: +86-15854209587, Email: jiasheng0813@163.com

working parts, with less effort on bearing parts optimization design. Especially, researches on the lightweight design for small-scale two-row peanut planting machines are rare.

In recent years, intelligent optimization algorithms that have been widely used in scientific research have seen rapid development in various disciplines. They are divided into swarm intelligence algorithms and genetic evolutionary algorithms[12,13]. Particle Swarm Optimization was proposed by Eberhart and Kennedy[14], which are widely introduced in various scientific research fields. In its development, optimization algorithms have achieved a combination with neural network algorithms. Compared with genetic algorithms, particle swarm optimization is more suitable for multi-objective optimization design due to its simplicity and strong optimization ability[15-17]. The Seagull Optimization Algorithm (SOA) is a new bio-inspired algorithm designed to solve complex optimization problems in group optimization[18].

Tsiptsis et al.[19] used particle swarm optimization to optimize 2D frame or frame tower structures, testing their sizes, shapes, and topology optimizations. The results showed that the PSO method can be flexibly applied to the optimization of both straight tower and curved tower structures. Omidinasab and Goodarzimehr[20] proposed an approach to design benchmark frame structures with discrete variables by combining hybrid Particle Swarm Optimization (PSO) and Genetic Algorithm (GA). Dhiman et al.[21] put forward the Evolutionary Multi-Objective Seagull Optimization Algorithm (EMoSOA) based on the Seagull Optimization Algorithm, which validated its efficacy for such designs as welding beam design, multi-disk clutch brake design, pressure vessel design, and bar frame design, which demonstrated the sufficiency of the Evolutionary Multi-Objective Seagull Optimization Algorithm for mechanical structure optimization. At present, intelligent optimization algorithms are more widely adopted in industrial fields such as pressure vessel design, gear reducer design, and automobile side collision design than that in agricultural machinery areas. By using the SOA algorithm and providing optimization boundary parameters based on its characteristics, lighter frame structure designs can be more quickly achieved.

Given the current development of peanut planting machines, this paper aims to finger out a feasible approach for planting machine lightweight design, which set a two-row small peanut planting machine as the research object. By combining SW software and ANSYS software, the framework structure of the machine is parameterized and modeled for the purpose to establish a 3D model of the peanut planting machine and an optimization model of the framework of the planting machine. ANSYS software is used to perform static structural analysis and sensitivity analysis on the framework, and the best solution is selected with the SOA optimization algorithm. Based on size and multi-objective optimization schemes, the peanut planting machine framework is designed to be lightweight.

2 Optimization of design goals and process

2.1 Optimization design goals

The optimization design process mainly includes such steps as designing the mechanical structure, determining the design variables, and objective functions, and establishing the 3D models[22]. The research is focused on small peanut seed drills in the Shandong area. The one-ridge two-row peanut seed drill is composed of multiple modules, including fertilization, seeding, pesticide application, trenching, ridge-making, and soil covering. The drill's frame which mainly consists of rectangular steel pipes welded with strip steel plates adopts an integrated frame structure. The material applied features Q235 with a yield strength of 235 MPa. Before finite element analysis for the peanut seed drill, its frame, and main components are parameterized and modeled by Solidworks three-dimensional drawing software. The model is shown in Figure 1. The detailed parameters of each component of the frame are listed in Table 1.

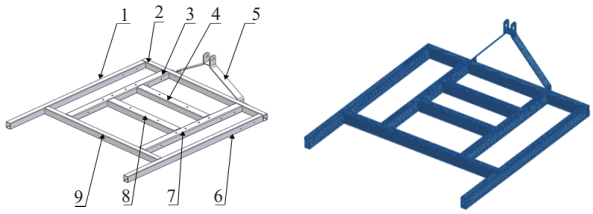

a. 3D model of peanut seeder frame b. Finite element model of the peanut planting machine frame

1. Left longitudinal beam 2.Front horizontal beam 3.Middle support left longitudinal beam 4. Middle support front horizontal beam 5. Three-point suspension assembly is welded with strip steel plates 6. Right longitudinal beam 7. Middle support right longitudinal beam 8. Middle support rear horizontal beam 9. Rear horizontal beam is welded with rectangular steel pipes

Figure 1 Peanut seeder machine frame model

Table 1 Parameters of the peanut seeder frame model

Materials	Specification/mm	Thickness/mm	Elastic modulus/MPa	Poisson ratio	Density/ kg·m^{-3}	Yield strength/MPa
Q235	40×60	5	2.01×10^{-5}	0.29	7850	235

2.2 Optimization design process

When conducting optimization design, the rack is first parametrically modeled. After completing the modeling, the model is subjected to static structural analysis and sensitivity analysis respectively. After the above steps are completed, the optimization goals and design variables are determined. The optimization goals and design variables are modeled for structural optimization, and then iteratively optimized using the SOA algorithm. After obtaining the optimal solution, finite element analysis is performed to verify whether the optimization results meet the design objectives. If the design objectives are met, the results are output and saved. If the goals are not achieved, the reasons are analyzed, and the optimization process is recalculated. The rack design flowchart is shown in Figure 2.

3 Mechanical structural analysis

3.1 Static mechanical structural analysis

To achieve better analysis results, and obtain a more accurate finite element model, while improving analysis calculation speed[23], the following simplification processes are taken into account on the frame without affecting the calculation accuracy: ignoring small local features such as mounting holes and chamfers; considering the frame materials to be uniform in density; connecting the frame components by welding, handling the welding seams with maximum strength and treating the frame parts as a whole. After importing the three-dimensional solid model created in Solidworks into ANSYS Workbench, Mesh was applied to mesh the model. The smaller the mesh size is, the higher the accuracy of the calculation turns out. The skew criterion[24] was followed during the process to ensure accuracy and mesh quality. The mesh size was set to 5 mm, and after division, the number of elements was 132 939 and that of nodes was 266 413.

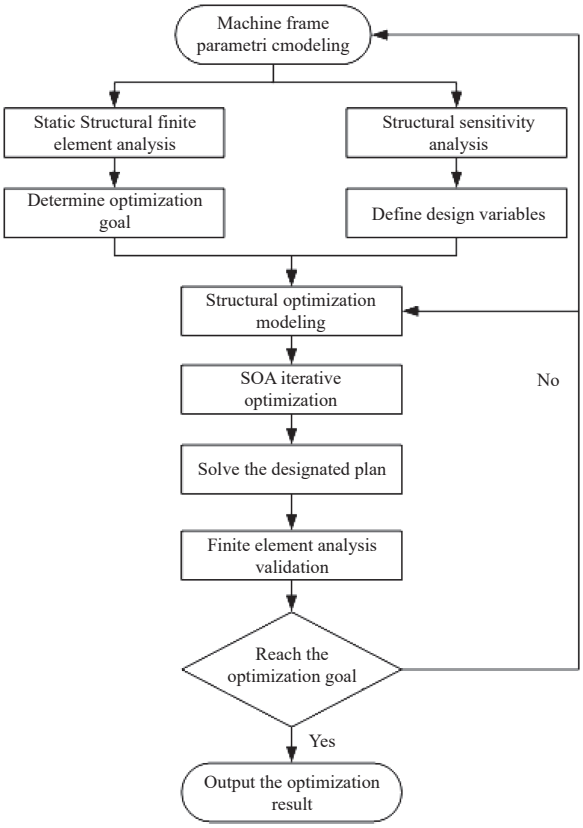

Figure 2 Optimized design process for the Frame

A static structure analysis was conducted on the original rack with external loads which is the main source of stress on the rack[25,26] and is generated from the rack's own gravity, planter weight, seed box, and fertilizer box weight as well as its additional weight. The total load of the rack is measured at 1550 N with a seed box load of 118 N and fertilizer box load of 206 N. The rack model is set with fixed constraints. Since the rack is connected to the tractor through a three-point suspension, the suspension device is fixedly constrained. It has been calculated that the maximum displacement of the rack is 0.2615 mm, which occurs at the rear crossbeam of the main frame and the rear part of the two longitudinal beams. While the maximum stress of the rack is 30.586 MPa. The static structural analysis of the rack is shown in Figure 3, and the maximum principal stress cloud map is displayed in Figure 4. As the yield strength of Q235 is 235 MPa, with a safety factor of n =1.2[27], the allowable stress of the material is calculated as 195 MPa according to Equation (1).

$$[\sigma] = \frac{\sigma_s}{n} \quad (1)$$

where, $[\sigma]$ is the allowable stress, MPa; σ_s is the material stress, MPa; n is the safety factor.

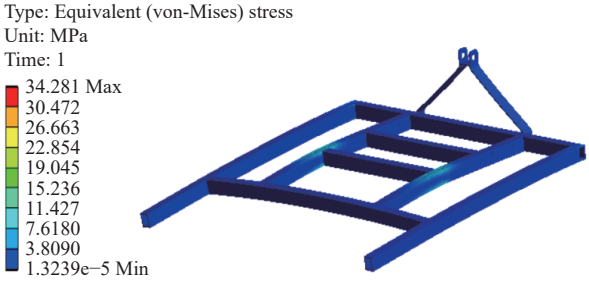

Note: Deformation is magnified by 400x.

Figure 3 Peanut seeder frame equivalent stress cloud map

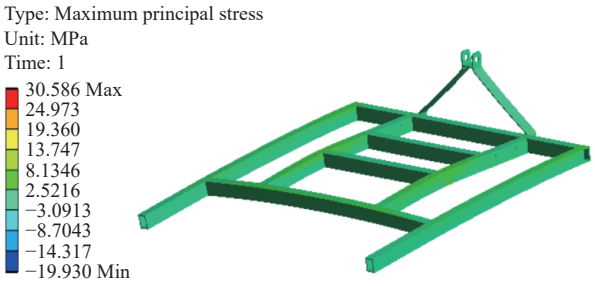

Note: Deformation is magnified by 400x.

Figure 4 Maximum principal stress cloud map of peanut seeder frame

3.2 Mode analysis

In dynamic analysis, modal analysis is an indispensable part of mechanical design. As a common approach to studying object vibrations, the determination of its natural frequency and vibration mode can avoid resonance, control noise and grasp the structure modal parameters in order to provide a reference for mechanical design[28,29]. Serving as a main carrier for the parts of peanut seeder, the frame operates through the three-point suspension of the tractor. Its excitation sources come from the engine frequency of the tractor and the random vibration frequency of the working land. Due to the changes in the working land, the main excitation is the engine frequency at an engine input speed of less than 50 Hz[30]. The natural frequency is a unique property of the material itself and is related to its own stiffness, mass, and other properties. Reducing the vibration frequency in mechanical structures and preventing resonance have become increasingly important in ensuring the service life of electromechanical components[31-33]. To avoid resonant phenomenon caused by the same frequency occurring between natural and external excitation frequencies after the structural optimization, fixed constraints are set after mesh division in ANSYS. Given that, the first-order method is adopted for modal analysis to obtain the top ten frequencies. The analysis results are listed in Table 2.

Table 2 Top ten modal frequencies of the peanut seeder

Order	Modal frequency/Hz	Vibration description
1	67.206	The main frame longitudinal beam bends up and down.
2	69.169	The lateral beams at the back bend upward.
3	102.44	The middle supporting longitudinal beam bends to the right.
4	109.06	The three-point suspension upper part bends.
5	113.53	The three-point suspension upper part twists inward.
6	173.80	The three-point suspension support plate bends outward.
7	185.24	The center part of the rear beam bends upwards.
8	192.84	The main frame longitudinal beam bends inward.
9	197.43	The main frame longitudinal beam bends left and right in the middle.
10	230.68	Main frame longitudinal beam center up and down bending.

Since the engine is the main source of vibration excitation of the frame during operation, the minimum input frequency of it is less than 50 Hz, which is different from the inherent frequency of the seeder frame so that no occurrence of resonance phenomenon will be in sight. When the engine is under load, its vibration frequency is positively correlated with its speed. The peanut seeder is suitable for small and medium tractors, with a maximum speed of 2400 r/min, a maximum of four cylinders, and a maximum stroke of four. The equation for calculating the engine vibration frequency is as follows:

$$f = \frac{2Mn_c}{60T} \tag{2}$$

where, M is the cylinder number of the engine; n_c is the engine speed, r/min; T is the engine stroke.

By substituting the relevant parameters into Equation (2), the calculated excitation frequency of the engine during load operation is 80 Hz. Upon comparison of the calculated result with the frame modal analysis, it can be seen that there is no overlapping of the engine excitation frequency and the frame's inherent vibration frequency. As there is a certain frequency interval between them, no resonance phenomenon will occur.

4 Frame structure sensitivity analysis

4.1 Determining optimization variables

Sensitivity analysis is a method by which the sensitivity of one parametric variable[34-35] to changes in other variables or parameters is studied. In mechanical structure optimization design, sensitivity analysis is used to select optimization variables and determine optimization objectives[36]. Through the study of the static structure of the peanut seeder frame, the main focus is on the sensitivity of the static structure rigidity for design parameters. The balance equation of the peanut seeder frame structure is:

$$k\delta = F \tag{3}$$

where, k is the stiffness, N/m; δ is the structural displacement, m; and F is the load vector, N.

Taking the derivative of the balance equation, the sensitivity of the displacement to the thickness d is

$$\frac{\partial \delta}{\partial d} = \frac{\Delta \delta}{\Delta d} = \frac{\delta(d+\Delta d) - \delta d}{\Delta d} \tag{4}$$

In the finite element analysis of the peanut seeder frame structure, the sensitivity is calculated mathematically and the parameters with larger impact factors are selected as design variables so as to optimize the structural optimization process. ANSYS is applied to classify and, with the optimal gradient method, calculate the optimization target area of the peanut seeder frame structure. The sensitivity curve of the thickness with respect to the rigidity deformation is obtained through comparative analysis, and the sensitivity curve is shown in Figure 5.

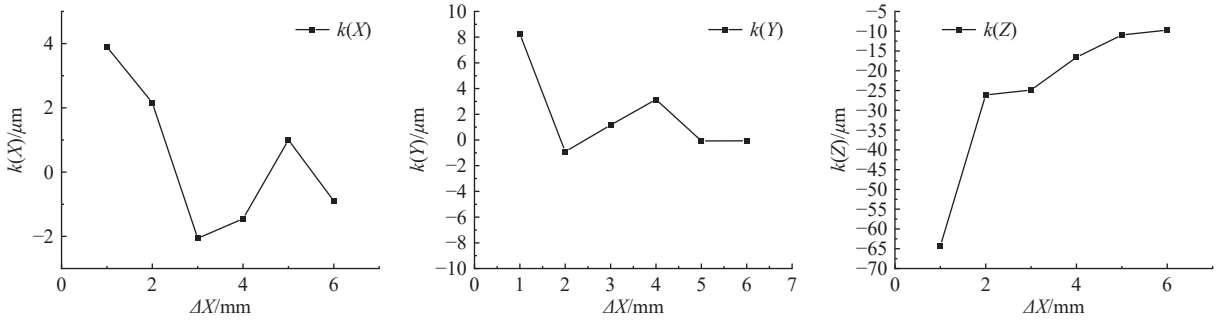

a. *X*-direction b. *Y*-direction c. *Z*-direction

Figure 5 Curves of stiffness versus thickness

From the analysis of material thickness sensitivity, it can be seen that the changes in material thickness have a significant impact on the deformation of stiffness. So for structural optimization, it is necessary to consider reducing the impact of stress on the structure after optimization.

4.2 Machine frame multi-objective optimization modeling and solution

The objective of this research is to find the optimal distribution solution with the minimum mass after meeting the strength and stiffness requirements for the seed drill frame to function. The three-point suspension of the seed drill was designed according to the national standard parameters of GB/T 1593-2015 (Agricultural Wheeled tractor—Rear-mounted three-point linkage—Categories 0, 1N, 1, 2N, 2, 3N, 3, 4N and 4)[37]. As the front beam of the frame is connected to the suspension by welding, the parameters of the frame' s main framework are subject to constraints from both welding dimensions. As a result, the internal structure beam area of the frame can be optimized, and 8 design variables have been defined as: front beam thickness x_1, rear beam thickness x_2, left beam thickness x_3, right beam thickness x_4, front beam height h_1, rear beam height h_2, left beam height h_3, and right beam height h_4, As the frame is designed symmetrically, the combination of the design parameters is $X = (h_1, h_2, h_3, h_4, x_1, x_2, \ldots x_8)$, the initial value of the rectangular steel tube wall thickness is x_i = 6 mm, and the initial value of the middle support beam height is h_i = 60 mm. The weight of the peanut seed drill frame is taken as the objective function. Thus, the optimized design mathematical model of the peanut seed drill frame structure is obtained:

$$\begin{cases} \min F_m(X) = f(x_1, x_2, x_3, x_4) \\ \min F_\delta(X) = f(x_1, x_2, x_3, x_4, x_5, x_6, x_7, x_8) \\ \text{s.t} \begin{cases} 2\text{ mm} \le x_i \le 6\text{ mm}, \quad i = 1,2,3,4,5,6,7,8 \\ 40\text{ mm} \le h_i \le 60\text{ mm}, \quad i = 1,2,3,4 \end{cases} \\ \sigma_{\max} \le [\sigma] = 195\text{ MPa} \end{cases} \tag{5}$$

where, $F_m(X)$ is the optimization objective function relative to mass for the design variable, kg; $F_\delta(X)$ is the optimization objective function for the maximum deformation of the frame, mm; x_i is the thickness of the i^{th} design variable, mm; h_i is the height of the i^{th} design variable, mm; $\sigma_{\max}$ is the maximum stress sustained by the frame, MPa; $[\sigma]$ is the allowable stress of the frame, MPa.

5 Multi-objective optimization based on SOA algorithm

In order to explore a more efficient and accurate optimization method for one-ridge two-row peanut seeders' frame structure, the SOA optimization algorithm was selected to upgrade the seeder frame, thereby providing ideas for the structural optimization of peanut agricultural machinery.

5.1 Optimization method of SOA algorithm

The SOA algorithm simulates both the optimizing process of searching and attacking by the population during migration and the individual's avoidance of collision during the movement of the population in attempt to calculate new positions with additional

variables:

$$\vec{C}_s(t) = A\vec{P}_s(t) \tag{6}$$

where, $\vec{C}_s(t)$ is a non-conflict position in the space; $\vec{P}_s(t)$ is the current coordinate; t is the current iteration; A is the current space population search movement behavior.

$$A = f_c - t\frac{f_c}{Max_{\text{iteration}}} \tag{7}$$

where, f_c is the control factor and $Max_{\text{iteration}}$ is the maximum number of iterations.

By introducing f_c, the frequency of variable A is linearly reduced to 0.

After resolving collisions between individuals in different populations, move and search towards the optimal coordinate direction in space.

$$\vec{M}_s(t) = B\left(\vec{P}_{bs}(t) - \vec{P}_s(t)\right) \tag{8}$$

where, $\vec{M}_s(t)$ is the optimal coordinate direction; B balances the search and development through random behavior.

$$B = 2A^2 r_d \tag{9}$$

where, r_d is a random number in the range [0, 1].

The final individual calculates the relative position of the optimal coordinates through updating the following Equation:

$$\vec{D}_s = \left|\vec{C}_s + \vec{M}_s\right| \tag{10}$$

where, $\vec{D}_s(t)$ is the distance between the search individual and the optimal search target.

The population generates a spiral movement during prey attack, and its behavior on the *XYZ* plane is as follows:

$$\begin{aligned} x &= r\cos(\theta) \\ y &= r\sin(\theta) \\ z &= r\theta \\ r &= ue^{\theta v} \end{aligned} \tag{11}$$

The algorithm adopts shape to control constant variables u and v, and calculates the spiral radius r; θ is a random number within [0, 2π], and e is the base of the logarithm of natural numbers.

$$\vec{P}_s(t) = \vec{D}_s(t)xyz + \vec{P}_{bs}(t) \tag{12}$$

Save the output of the best solution $\vec{P}_s(t)$ and updates the new positions of other individuals.

5.2 SOA algorithm optimization process

The SOA algorithm flowchart is shown in Figure 6.

(1) For the optimization goal, the initial parameters are input, such as x_i, h_i, etc. The initial value of parameter iteration is set as l=0 and the maximum number of iterations as t.

(2) Introduce the objective function and initialize the population X_b (b=1, 2, …, n), calculate the population position, individual position, and fitness based on Equations (6) and (7).

(3) The speed and position of each individual are calculated and updated through iteration based on Equation (10). Due to the influence of material processing technology and its standards, the search should be close to integers within the optimization range.

(4) The fitness value of each individual is calculated through the objective function. During the optimization of the algorithm, a penalty function is introduced to classify individuals, where the fitness of individuals that do not meet the constraint conditions is 0 and the constraint problem is converted into an unconstrained one. The penalty function is as follows:

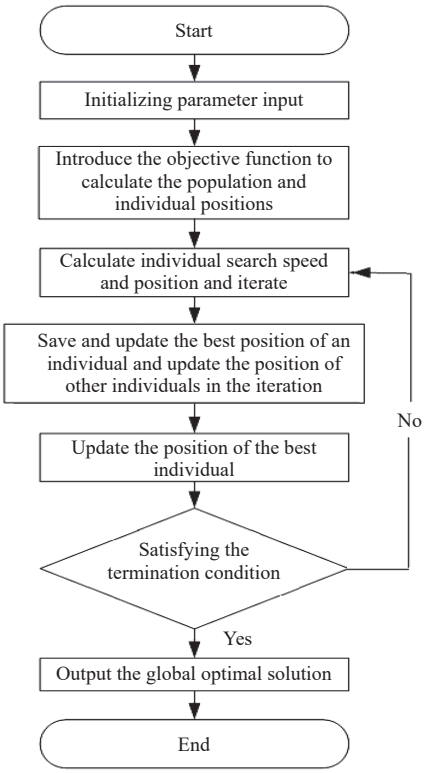

Figure 6 SOA algorithm flowchart

$$P(x) = \sum_{i=1}^{m}(\alpha \max(0, g_i(x)))^{\beta} \tag{13}$$

(5) The individual's current fitness value is compared and updated. First, it is compared with the best value in its own database, and the superiority is judged and the best value is updated in the database. Secondly, the individual's current best value is compared with the globally recorded one to judge its superiority. And the best value after the comparison is recorded and updated.

(6) Save the optimal value, then determine if the optimization termination condition has been met, if it does then output, otherwise re-enter the operation.

In this iteration of the SOA, the population size is set to 100. The maximum number of iterations $Max_{\text{iteration}}$ is 200, while the dimension is 4, i.e. X_1-X_4. The upper boundary is set to l_b=[6, 6, 60, 60], and the lower boundary is set to u_b=[3, 3, 40, 40]. After iteration, the population converges and the convergence of iteration optimization is shown in Figure 7.

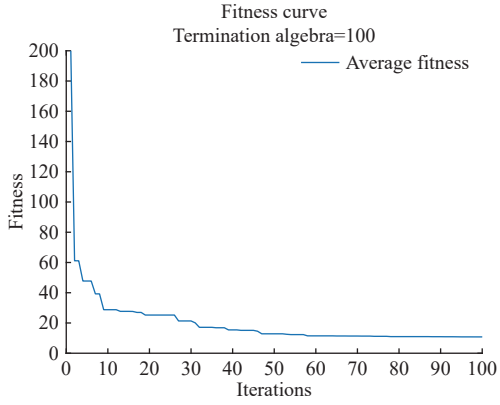

Figure 7 SOA algorithm iteration process

As shown in Figure 8, during the optimization process, the best solution iteration process can determine the optimal solution numerical value. By combining the corresponding best solution

candidate points, it can be concluded that the optimal solution for rod thickness is 3.1 mm when convergence is reached. The optimal solution for rod height is 40.9 mm when convergence is attained. By processing the optimization results, the mass, volume, and modal frequency of the optimized frame are normalized to verify the optimization results.

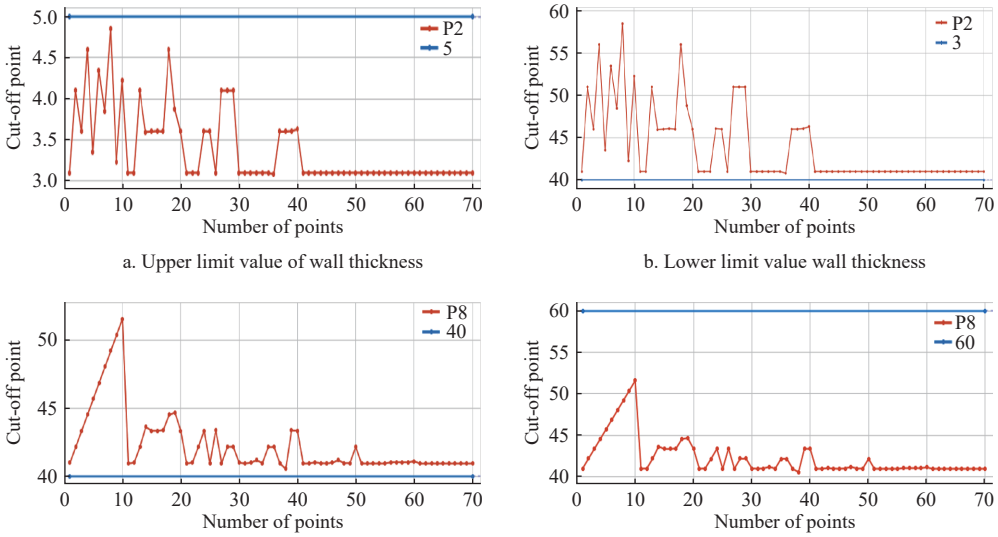

a. Upper limit value of wall thickness

b. Lower limit value wall thickness

c. Lower limit value of height

d. Upper limit value of height

Figure 8 Optimal solution iteration process

Both the normalized processing graph in Figure 9 and the frame mass response surface graph in Figure 10 show that the fit of the optimized objective value is relatively smooth, which implies a good normalization. The trend of the response surface graph is relatively smooth, indicating that the optimization of the peanut planting machine frame is effective.

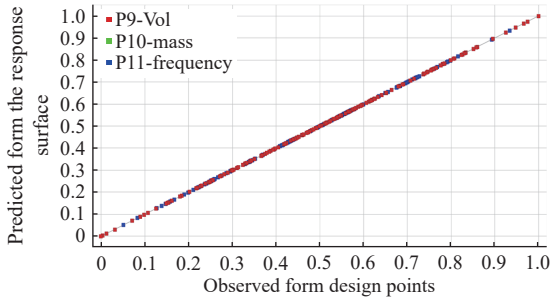

Figure 9 Normalization process after optimization

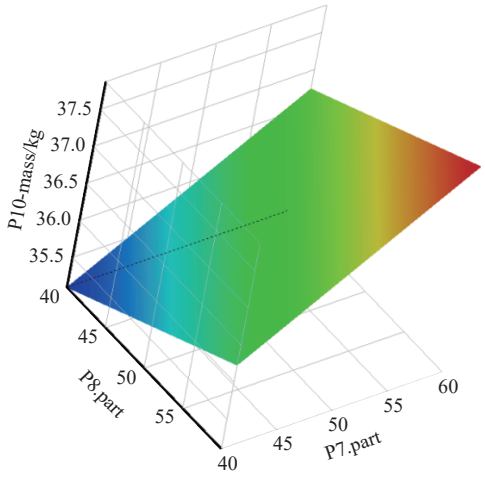

Figure 10 Mass response surface plot after optimization

According to the optimal derounding and rounding size value of Table 3, the seeder frame was re-parameterized, and the structure diagram of the planter frame after optimization was obtained, as shown in Figure 11. The middle support longitudinal beam was a 40 mm×60 mm rectangular steel pipe with a wall thickness of 6 mm before the weight reduction, the wall thickness was changed from 6 mm to 3 mm after weight reduction and the external dimensions remained unchanged.

Table 3 Dimension values before and after optimization

Part number	Before optimization	After optimization
1/6	6 mm	3 mm
2/9	6 mm	3 mm
3/7	6 mm	3 mm
4/8	6 mm	3 mm
3/7	60 mm	40 mm
4/8	60 mm	40 mm

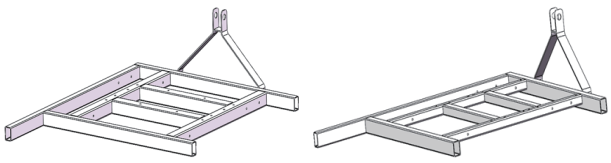

a. Structure diagram of the front frame for weight reduction optimization

b. Frame structure diagram after weight reduction optimization

Figure 11 Comparison of peanut seeder frames before and after optimization

According to the fourth strength theory, the equivalent stress is used as the basis for determining the yield failure stress of the material, and the maximum principal stress is used as an auxiliary judgment standard. The optimized static structural stress distributions are shown in Figures 12 and 13. It can be seen that the optimized equivalent stress and maximum principal stress are still lower than the allowable stress value. As listed in Tables 4 and 5, the weight of the optimized frame has been reduced from 52.0 to 35.1 kg, decreased by 32.5%. The modal vibration frequency has been reduced from 67.206 to 53.56 Hz, which is still higher than

theengine input speed and does not cause resonance under the requirement of ensuring the overall rigidity of the frame structure.

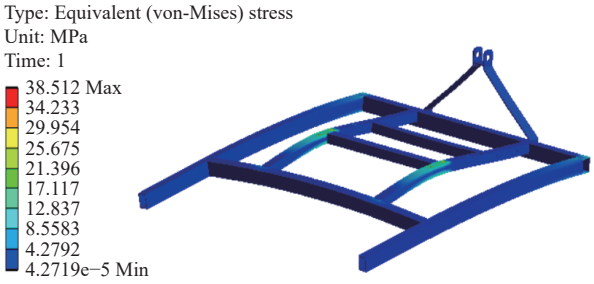

Figure 12 Equivalent stress cloud map of peanut seeder frame after optimization(Deformation is magnified by 400x)

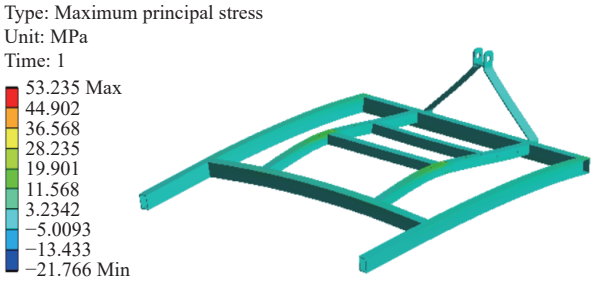

Figure 13 Maximum principal stress cloud map of peanut seeder frame after optimization (Deformation is magnified by 400x)

Table 4 Parameter values of optimized seeder frame

Item	Before optimization	After optimization
Total mass/kg	52	35.1
Maximum deformation/mm	0.261	0.528
Equivalent (von-Mises) stress/MPa	34.281	38.512
Maximum principal stress/MPa	30.586	53.235

Table 5 Intrinsic frequencies of optimized peanut seeder frame

Order	1	2	3	4	5
Modal frequency/Hz	53.56	56.94	90.45	108.49	113.51
Order	6	7	8	9	10
Modal frequency/Hz	165.72	173.79	194.09	199.79	228.73

6 Field tests

To verify the stability and reliability of the peanut seeder frame, as well as the working performance of the entire machine after lightweight, an electric driven precision peanut seeder was installed on the optimized one row and two rows peanut seeder as a platform for field seeding experiments. The experimental site is located in the experimental field of Laixi City, Qingdao City, Shandong Province, as shown in Figure 14. Furthermore, a research group's electrically driven precision peanut planter was installed on the left side of the peanut planter while a common ground-driven peanut planter on its right so that a more accurate comparative test could be acquired. Components such as soil covering and film covering of the peanut planter were removed in order to reduce the influence of human factors.

By applying GB/T 6973-2005 (Testing methods of single seed drills-precision drills)[38] and NY/T 503-2002 (Operating quality of single (precision) seeder for intertilled crops)[39] as evaluation criteria, such experiments were conducted as on a peanut seeder to assess the effect of seeding speed against row spacing stability; on the effect and pattern of row spacing stability in seeding driving mode; on determination of row spacing acceptance, miss-seeding and double-seeding rates.

Figure 14 Field test

The test parameters are based on the Shandong region peanut planting agronomic standards and NY/T 2404-2013 (Technical regulations for high yield cultivation of peanut by single-seed and precision sowing method)[40], such as the seeding depth is 2-3 cm, the row spacing is generally 15-27 cm and the working speed generally 2-5 km/h. The test row spacing is set at three levels of 16 cm, 21 cm, and 27 cm respectively, while the seeding speed is at two levels of 2-3 km/h and 3-4 km/h.

6.1 Testing methods

6.1.1 Test on the influence of sowing speed on the stability of plant spacing

To explore the impact made by sowing machine on stability of row spacing at various sowing speed, different sowing row spacing conditions are set, which repeated for 3 times at the working speed of the sowing machine of 2-3 km/h and 3-4 km/h. A single test with 250 seeds is conducted to continuously measure the row spacing.

6.1.2 Effect of different driven seed meters on plant spacing stability and field test

Experiments that are aimed at exploring the influence and pattern of different types of seed metering devices with different driving modes on the stability of plant spacing in peanut sowing machines were conducted with ground-wheel-driven and stepper motor-driven seed metering devices. The sowing row spacing was set at 16 cm, 21 cm, and 27 cm, repeating three times with operating speed of the seeder at 2-3 km/h and 3-4 km/h. The continuous measurement of spacing between seeds was carried out for a total of 250 seeds in a single experiment.

6.1.3 Determination of the rate of row spacing compliance, skipping rate, and double-seeding rate

Seeder performance was verified through field tests which were conducted with the seeder traveling at normal working speed (≤5 km/h) and row spacing set to 16 cm, 21 cm, and 27 cm, collecting a total of 250 groups of experimental data. The actual seed spacing average value $\bar{L}$ (m), seed spacing compliance index L_q(%), skippage rate M(%), and double seed rate R(%) were obtained as the results of

field experiments. The calculation Equation is as follows:

$$\begin{cases} \bar{L} = \dfrac{L}{N_z} \\ L_{\mathrm{q}} = \dfrac{N_L}{N_z} \times 100\% \\ M = \dfrac{N_{\mathrm{m}}}{N_z} \times 100\% \\ R = \dfrac{N_{\mathrm{r}}}{N_z} \times 100\% \end{cases} \tag{14}$$

where, N_z is the total number of measurements, in this experiment N_z =250; L is the measured plant spacing, m; N_L is the number of plant spacings that are qualified ($0.5L_a \leq L \leq 1.5L_a$); N_m is the total number of missed seeds ($L>0.5L_a$); N_r is the number of re-seeded seeds ($L<0.5L_a$); L_a is the set plant spacing, m.

6.1.4 Determination of the rate of seeding depth compliance

To verify the seeding depth effect of the seeder, the seeding depth is set to be greater than or equal to 3 cm with an error tolerance of ±1 cm as the qualified seeding depth. When the seeding depth is less than 3 cm, an error of ±0.5 cm is considered as the qualified. The sowing depth of peanuts is set to 3 cm, and the sowing depth error is set to ±1 cm.

On the working plot, 5 small areas are selected according to technical specifications and requirements. Each area has one working width and a length of 2 m. The soil layer of the sowing row is cut open and the thickness of the layer covering the seed is measured. Five points are measured in each row for each area. The sowing depth pass rate of each area its average value is calculated. The equation is as follows:

$$H = \frac{h_1}{h_2} \times 100\% \tag{15}$$

where, H is the seeding depth pass rate in percent; h_1 is the number of seeding depth pass points; h_2 is the total number of points tested.

6.2 Test results and analysis

6.2.1 Testing and analysis of the seeding speed's impact on row spacing stability

As shown in Table 6, the test results indicate the effects of seeding speed on the stability of plant spacing, showing that seed spacing within ±0.5 times of the set spacing is considered as qualified seeding. As can be seen from the table, the seed spacing of 16 cm and 21 cm has better results and the plant spacing qualified rate is around 97%, with little impact from the working speed. However, when the plant spacing is 27 cm, the qualified rate is inversely proportional to the working speed, but the qualified rate still remains above 96%. Thus, it means that the seeder machine has a high stability at different speeds.

Table 6 Results of the planting speed's impact on row spacing stability

Workingspeed/ km·h^{-1}	Set spacing/cm	Actual average spacing/cm			Qualified spacing rate/%		
		1	2	3	1	2	3
2-3	16	16.30	16.06	16.50	98.83	98.32	98.99
	21	21.49	21.19	21.31	98.01	98.10	97.50
	27	28.70	26.89	28.00	97.89	98.21	98.35
3-4	16	15.80	16.15	15.90	98.98	98.30	98.61
	21	21.60	20.90	21.32	98.61	98.89	98.34
	27	28.81	28.34	28.91	97.32	96.94	96.92

6.2.2 Effect of different seeding mechanisms with various driving modes on plant spacing stability and testing results analysis

As shown in Table 7, when the seeding distances were 16cm and 21 cm with the speed at 2-3 km/h, the seeding qualification rate was above 96% even in different driving modes of the seeder. However, with the increase of working speed and seeding distance, the seeder's qualified rate in wheel-driven mode decreased significantly (from 98.60% to 85.34%). The motor-driven mode, by contrast, was less affected by the forward working speed and seeding distance. The optimized frame of the seeder has a small effect on the stability of seeding distances when different driving modes of seeder are put into operation, and the seeder's reliability is relatively high.

Table 7 Comparison test results of mechanical peanut seeder

Working speed/km·h^{-1}	Setspacing/ cm	Actual average spacing/cm		Qualified spacing rate/%	
		Ground wheel	Stepper motor	Ground wheel	Stepper motor
2-3	16	16.53	16.82	97.22	97.33
	21	20.55	21.55	96.51	97.89
	27	29.46	28.01	85.94	96.82
3-4	16	15.95	16.32	95.04	97.98
	21	22.20	21.90	90.53	98.80
	27	29.89	28.92	85.34	98.05

6.2.3 Experimental results and analysis of plant spacing accuracy, seed missing rate, and seed over-planting rate of the seeder

As shown in Table 8, the average pass and missing rates are 98.06% and 1.30% respectively under the set row spacings and working speeds. When the sowing machine operates at medium and low speeds (2-3 km/h, 3-4 km/h), the impact on the pass rate of row spacings is relatively small with pass rates around 98%. This indicates that the optimized machine has a good sowing effect and sound compatibility for seeding sowers.

Table 8 Performance table of the seeder field test

Working speed/ km·h^{-1}	Seed spacing/ cm	Actual spacing/ cm	Qualification rate/%	Miss-seeding rate/%	Reseeding rate/%	Coefficient of variation/%
2-3	16	16.52	98.26	1.12	0.62	13.64
	21	21.50	97.82	1.25	0.93	15.68
	27	27.80	98.10	1.22	0.68	17.96
3-4	16	16.05	98.39	1.15	0.46	11.70
	21	21.34	98.62	1.08	0.30	18.43
	27	28.05	97.22	1.89	0.89	28.72

6.2.4 Testing results and analysis of the rate of seeding depth compliance

As shown in Table 9, the sowing depth qualification rate is measured according to the specification requirements, of which JB/T 10293-2013 "Single Grain (Precision) Seeder Technical Conditions" stipulates that the sowing depth qualification rate is not less than 80%, and NY/T 3660-2020 "Peanut Seeder Operation Quality" stipulates that the sowing depth pass rate is ≥ 85.0%, so the parameter value of the sowing depth pass rate is set to ≥85%. In summary, it can be obtained that the test data show that the average sowing depth qualification rate of the seeder after weight reduction is 92%, the peanut seeder is relatively stable in reducing the sowing depth, the working performance of the seeder is reliable and the weight reduction has little effect on the sowing depth, and the comprehensive operation effect of the soil covering and suppression device is better to meet the agronomic requirements.

The field test results demonstrated that the machine frame can perform precision sowing of peanuts well when it is equipped with different driving mechanisms and operates at different sowing

speeds. Given that, it turns out to be more suitable for low to medium speed operations in small planting areas.

Table 9 Table of seed planting depth pass rate determination

Measure the number of sections	Length/ Sowing depth	Number of rows	Measurement point					Planting depth pass rate/%
			1	2	3	4	5	
1	2 m/3 cm	1	2.5	3.1	3.2	3.4	4.2	90%
		2	3.4	3.5	3.7	3.9	3.5	
2	2 m/3 cm	1	3.4	4.5	3.5	3.2	2.8	90%
		2	2.9	2.7	3.1	3.3	2.9	
3	2 m/3 cm	1	3.4	3.5	3.7	2.9	2.7	90%
		2	2.9	2.7	2.9	3.2	4.1	
4	2 m/3 cm	1	2.5	3.1	2.7	2.6	2.9	90%
		2	3.2	3.3	2.9	3.8	4.2	
5	2 m/3 cm	1	2.9	2.6	3.5	3.2	2.9	100%
		2	3.6	3.8	3.4	3.5	3.2	

7 Conclusions

(1) The main carrier frame of a one-ridge two-row peanut sowing machine is taken as the research object in this paper. A multi-objective optimization mathematical model is established, and a structural optimization design method based on a SOA intelligent optimization algorithm is applied to optimize the structure of the peanut sowing machine frame in order to achieve the goal of lightweighting the frame structure.

(2) Based on the size of the peanut sowing machine frame, a finite element model is established and analyzed, providing a basis for static structural analysis and lightweight optimization design.

(3) The lightweight design effectively reduced the weight of the peanut sowing machine frame, resulting in a reduction of the frame weight from 52 to 35.1 kg. The modal frequency was reduced from 67.206 to 53.56 Hz, and the maximum deformation was 0.528 mm. The optimization goal of lightweighting was achieved while satisfying the allowable stress requirements without causing resonance, improving the static stability and meeting the design and use requirements.

(4) Field tests have shown that when operating at different speeds according to the test settings, the qualified rate of row spacing is ≥96%, and the miss rate is <2%. The prototype working condition is good at different speeds, and has little effect on qualified rates of row spacing. When using different types of seeders in different driving modes for planting, the prototype structure has no adverse effects on the agronomic requirements of row spacing and seeding depth. The qualified rate of seeding depth is ≥90%, and the average qualified rate is 92%. The seeding depth is stable, and the lightweight design of the frame did not cause a decrease in pass rate or stability during field tests. The working performance is reliable.

This research can achieve the lightweighting of a peanut seeder that can plant two rows at once, and achieve uniform planting in a small-scale planting mode. Due to the impact of various factors in field operations, such as planting height, soil viscosity, peanut variety, and other uncontrollable factors, the impact of the interaction between these factors on the overall performance of the seeder still needs to be studied.

Acknowledgements

This work was financially supported by the National key R&D plan (Grant No. 2022YFD2300101) and Shandong Peanut Industry Technology System Construction Plan (Grant No. SDAIT-04-09).

[References]

[1] Rosenthal S, Maaß F, Kamaliev M, Hahn M, Gies S, Tekkaya A E. Lightweight in automotive components by forming technology. Automotive Innovation, 2020; 3(3): 195–209.

[2] Wang M. Structure analysis and optimization of the frame of a electric patrol vehicle. Qilu University of Technology, 2020. (in Chinese)

[3] Liao Y, Liao B. Finite Element Analysis and Lightweight Design of Hydro Generator Lower Bracket. Manufacturing Technology, 2020; 20(1): 66–71.

[4] Yang Z, Deng B, Deng M, Sun G, Sung W P, Han T Y. A study on finite element analysis of electric bus frame for lightweight design. Proceedings of the MATEC Web of Conferences, 2018. EDP Sciences. doi: 10.1051/matecconf/201817503049.

[5] Cicconi P, Landi D, Germani M. An ecodesign approach for the lightweight engineering of cast iron parts. The International Journal of Advanced Manufacturing Technology, 2018; 99: 2365–2388.

[6] Luo W, Zheng Z, Liu F, Han D, Zhang Y. Lightweight design of truck frame. Proceedings of the Journal of Physics: Conference Series, F, 2020. IOP Publishing.

[7] Zhao L, Ma J, Wang T, Xing D. Lightweight design of mechanical structures based on structural bionic methodology. Journal of Bionic Engineering, 2010; 7(4): S224–S231.

[8] Cao S A, Chu J, Hao J, Hu C. Structure optimization of middle driving drum frame of belt conveyor. Coal Mine Machinery, 2022; 43(11): 132–134. (in Chinese)

[9] Chen S, Han H, Lu Q. Modal analysis of header for type 4LZ 2. 0 combine harvester. Transactions of the CSAM, 2012; 43(S1): 90–94. (in Chinese)

[10] Liao Y, Liu S, Sun Y, Ma Q, Lin M. Structural optimization for rack of cassava harvester based on sensitivity analysis. Transactions of the CSAM, 2013; 44(12): 56–61, 51. (in Chinese)

[11] Zhou M, Zhang L, Chen Y, Liu M, Huang Y. Structural optimization for rack of boat-type tractor based on sensitivity analysis. Transactions of the CSAE, 2016; 32(12): 54–60. (in Chinese)

[12] Goldberg D E, Holland J H. Genetic algorithms and machine learning. Machine Learning, 1988; 3(2-3). doi: 10.1023/A:1022602019183.

[13] Kirkpatrick S, Gelatt C D, Vecchi M P. Optimization by simulated annealing. Science, 1983; 220(4598): 606–615.

[14] Eberhart R, Kennedy J. A new optimizer using particle swarm theory. Proceedings of the Sixth International Symposium on Micro Machine and Human Science, IEEE, 1995.

[15] Li G Q, Yuan C, Wang S, Mao B, Dong Z L. Structural design of compound hydraulic swing cylinder based on co-evolution multi-objective genetic algorithm. Journal of Ship Mechanics, 2022; 26(11): 1694–1704. (in Chinese)

[16] Liu Y. Research on structural optimization design system based on parallel optimization algorithm. University of Electronic Science and Technology of China, 2021. (in Chinese)

[17] Lei M. Structure optimization design of RV reducer based on genetic algorithm and BP neural network. Lanzhou University of Technology, 2021. (in Chinese)

[18] Dhiman G, Kumar V. Seagull optimization algorithm: theory and its applications for large-scale industrial engineering problems. Knowledge-Based Systems, 2019; 165: 169–196.

[19] Tsiptsis I N, Liimatainen L, Kotnik T, Niiranen J. Structural optimization employing isogeometric tools in particle swarm optimizer. Journal of Building Engineering, 2019; 24: 100761.

[20] Omidinasab F, Goodarzimehr V. A hybrid particle swarm optimization and genetic algorithm for truss structures with discrete variables. Journal of Applied and Computational Mechanics, 2020; 6(3): 593–604.

[21] Dhiman G, Singh K K, Slowik A, et al. EMoSOA: A new evolutionary multi-objective seagull optimization algorithm for global optimization. International Journal of Machine Learning and Cybernetics, 2021; 12: 571–596.

[22] Chau N L, Dao T-P, Nguyen V T T. An efficient hybrid approach of finite element method, artificial neural network-based multiobjective genetic algorithm for computational optimization of a linear compliant mechanism of nanoindentation tester. Mathematical Problems in Engineering: Theory, Methods, and Aplications, 2018. doi: 10.1155/2018/7070868.

[23] Wang T. Finite element analysis and optimization design of the frame of a typed heavy truck. Dalian Jiaotong University, 2020. (in Chinese)

[24] Dao T-P, Huang S-C. Design and multi-objective optimization for a broad self-amplified 2-DOF monolithic mechanism. Sādhanā, 2017; 42: 1527–1542.

[25] Han Y. Finite element analysis and optimization design of the frame of a typed light truck. Dalian Jiaotong University, 2019. (in Chinese)
[26] Zhao C, Zhang C, Li Y, Bo C, Hao G, Dou H. Design and optimization of the frame of the air-driven electrostatic spray locomotive. Proceedings of the Journal of Physics: Conference Series, F, 2020. IOP Publishing.
[27] Pu L G. Mechanical principles and mechanical design series textbooks for the twelfth five-year plan of higher education undergraduate program textbooks for mechanical design. 9th Edition. Beijing: Higher Education Press, 2015. (in Chinese)
[28] Zhang Y, Zheng Z, Liu N, Han D, Meng H, Xia Q. Modal research on car aluminum alloy bumper beam based on finite element analysis and experiment. Machine Design and Manufacturing Engineering, 2022; 51(3): 73–78. (in Chinese)
[29] Zhi J, Zhang H, Wang Z, Zhang X, Ren Y, Zhao W. Finite element modal analysis and test of the whole concrete pump truck. Chinese Journal of Construction Machinery, 2021; 19(6): 549–554. (in Chinese)
[30] SCIENCES C A O A M. Agricultural machinery design manual. Beijing: China Agricultural Science and Technology Press, 2007. (in Chinese)
[31] Jin X, Chen K K, Ji J T, Zhao K X, Du X W, Ma H. Intelligent vibration detection and control system of agricultural machinery engine. Measurement, 2019; 145: 503–510.
[32] Jin X, Cheng Q, Tang Q, Wu J, Jiang L, Wu C Y, et al. Research on vibration reduction test and frame modal analysis of rice transplanter based on vibration evaluation. Int J Agric & Biol Eng, 2022; 15(4): 116–122.
[33] Niu P, Chen J, Zhao J D, Luo Z Y. Analysis and evaluation of vibration characteristics of a new type of electric mini-tiller based on vibration test. Int J Agric & Biol Eng, 2019; 12(5): 106–110.
[34] Ma Y, Wang X, Zuo W. Analytical sensitivity analysis method of cross-sectional shape for thin-walled automobile frame considering global performances. International Journal of Automotive Technology, 2020; 21: 1207–1216.
[35] Chai G, Huang S, Yue W, Yang G, Liang X, Shu G. Optimal design for torsional vibration damper based on sensitivity analysis. Transactions of the CSAE, 2009; 25(5): 105–108. (in Chinese)
[36] Hua Y, Zhu H, Gao M, et al. Multiobjective optimization design of permanent magnet assisted bearingless synchronous reluctance motor using NSGA-Ⅱ. IEEE Transactions on Industrial Electronics, 2020; 68(11): 10477–10487.
[37] GB/T 1593-2015. Agricultural Wheeled tractor—Rear-mounted three-point linkage—Categories 0, 1N, 1, 2N, 2, 3N, 3, 4N and 4. Inspection and Quarantine of the People's Republic of China; Standardization Administration of the People's Republic of China, 2015. (in Chinese)
[38] GB/T 6973-2005. Testing methods of single seed drills (precision drills) Inspection and Quarantine of the People's Republic of China; Standardization Administration of the People's Republic of China, (in Chinese)
[39] NY/T 503-2002. Operating quality of single (precision) seeder for intertilled crops. 2002. (in Chinese)
[40] NY/T 2404-2013. Technical regulations for high yield cultivation of peanut by single-seed and precision sowing method. 2013. (in Chinese)